BIOMEDICAL ENGINEERING 2022

Closed-loop control of a network of intra-muscular electrical microstimulators aiming for precise gestures: preliminary assays in New Zealand white rabbits

Álvaro Martínez Marco

upf. Universitat Pompeu Fabra Barcelona

Closed-loop control of a network of intra-muscular electrical microstimulators aiming for precise gestures.

Preliminary assays in New Zealand white rabbits

Álvaro Martínez Marco

Bachelor's thesis UPF 2021/2022

Thesis supervisors:

Dr. Antoni Ivorra

Marc Tudela-Pi

Dr. Jesús Minguillón

Dedicatory

To my beloved family, who has been from the distance outstanding support in every goal I have been chasing since I left my hometown, Soria. My dad for never letting me quit a personal project, my mum for her strong personality since I was little, encouraging me incessantly.

To Polytechnical School group of friends, with the ones I have had the pleasure to share academic quality time as well as joy. They got me to pursue my biggest version. Ultimately, to every single Professor that shed passion while teaching what is not written in the Literature.

Thankful to all the souls involved in my personal growth.

Acknowledgments

At first, I would like to make extensible my deepest gratitude to my PhD supervisors Prof. Antoni Ivorra, Jesús Minguillón and Marc Tudela-Pi for their continuous support and guidance as well as their initial trust vote towards me to conduct this thesis in the exciting electrical stimulation field.

I would like to express gratitude as well to Laura Becerra and Albert Comerma for their assistance to experimental sessions and the shared discussions in which key leads for the project were found.

To Gil Serrancolí and Ignasi Bellafont for the feedback in musculoskeletal modeling and controllers in contrasted softwares. To my friend Àlex Cánovas as well for his opinions and aid when designing the 3D printed elements.

I would like to send thanks especially to Marc for his inputs, his guidance, his patience.

Abstract

Functional electrical stimulation consists of the delivery of electrical pulses aimed to restore functional movements in paralytic individuals. Its level of applicability is still highly dependent on the invasiveness of the systems required to perform multi-site stimulations. In this framework, one of the most promising approaches is based on the deployment of wireless networks of intra-muscular microstimulators. However, up to date, this approach has been limited by the size of the currently available microstimulators.

Biomedical Electronics Research Group (BERG) at University Pompeu Fabra is pioneering the development of intra-muscular microstimulators with unprecedented features regarding minimal invasiveness. These devices have a diameter below 1 mm and most of their body is made up of flexible materials.

These injectable flexible devices developed by BERG, known as eAXONs, evoke neuromuscular stimulations using the rectification of volume conducted high frequency (HF) current pulses supplied by an external unit. Several of these independent eAXONs microstimulators can form a network to be implanted and ultimately, digitally controlled. Until now, BERG has manufactured and validated its first functional prototypes.

Nonetheless, their applicability to induce precise movements has still not been demonstrated. In this context is where the current Bachelor Thesis has its core hypothesis proposal: to prove that using a closed-loop controller and a network of implanted eAXONs it is possible to control certain precise muscular trajectories of 1 degree of freedom (DOF) in a New Zealand anesthetized rabbit. In order to find an appropriate deployment of these prototypes in a living organism, apart from the Simulink plant and the eAXONs technology, the thesis has integrated a 3D-printed exoskeleton architecture, a detailed stimulation protocol, a proper conditioning of the electronic system and the future lead of a predictive musculoskeletal model allowing for a deeper in-silico understanding of the evoked trajectories and the ultimate proof of the above mentioned core hypothesis.

Keywords

Functional electrical stimulation

Muscular restoration

Closed-loop controller

Electronic injectable device

Index

1. Introduction

1.1. Framework: Functional Electrical Stimulation and eAXONs Project

Electrical stimulation is a method that pursues the restoration of peripheral nerve mediated labors in individuals that got affected by a nervous system disorder. However, the stimulation can be based on different architectures such as percutaneous, superficial or implantable, being the last one the golden choice for long-term purposes. Indeed, the extent of its applicability is highly dependent on the degree of invasiveness required for its performance. Besides, apart from the vastly known limitation of the miniaturization of the devices performing the stimulations, there is an added one that can be considered the main thread to be solved in the current thesis.

1.1.1. The identified controller problem

One of the most challenging tasks in Functional Electrical Stimulation (FES) is the development of a controller accounting for the variant nonlinear neuromusculoskeletal system dynamics. Nowadays, current FES configurations are mostly based on an open-loop architecture, which has found large applicability and acceptance in clinics. These open-loop FES systems manually deal with stimulation parameters (e.g. pulse width) in a way that they do not include correction mechanisms (e.g. muscle biofeedback, joint mechanical response outputs). Therefore, they have scarce or directly lack from feedback information that may help fine-tune the parameters and allow for optimized performance metrics. Strategies based on open-loop architectures usually lead to fast muscle fatigue processes [1][2] since they evoke muscle contractions in a persistent basis thanks to implanted or cutaneous electrodes.

In this context, since muscular units show time-varying and external disturbances as well as non-linearities, the open-loop controllers hardly achieve precise control of subject's movements. Here, some alternatives such as neural network sliding mode control based on genetic algorithms (GAs) have been successful on controlling electrical stimulations and, ultimately, get the desired joint gesture. The main reason for closed-loop FES Systems to be rarely commercially distributed might be the difficulty on deploying a control architecture with a broad applicability to these non-linearities and time-varying muscle behaviors.

1.1.2. The proposed solution for the control

Having arrived to this point, an improvement on the stability and a minimization of the muscle fatigue is desired. The solution for them both is based on a closed-loop feedback controller where stimulation intensity has the possibility to get turned off or down when needed, as well as show better tracking performance and smaller sensitivity to modeling errors or what is the same, better adaptivity in modeling, parameter fluctuations or external noise and disturbances [3]. This way, it would be possible to fight back and overcome the drawbacks [4][5][6] that still arise in open-loop FES systems. Indeed, these disturbances and non-linearities are the factors that force the FES method to be very efficient if a proper restoration of hindlimb gestures and motions is desired (e.g. hand grasping, standing or walking).
What is more than clear is that a feedback loop may help when getting finer and more flamboyant control over the animal's limb trajectory. Even though many benefits are attributed to them, only open-loop controllers have made it to the market.

1.1.3. The identified bulky configuration problem

Seeking to obtain stable gestures in an animal hindlimb, the proposed solution of a closed-loop controller needed to be combined with the devices themselves acting upon the muscles. The whole set-up composed of the remote electrodes wired to the central stimulation unit is called implantable system. However, it is not a proper solution in all the cases; indeed, when the hindlimbs are to be individually stimulated in different muscular locations and concomitantly, an underlying complex surgery and a bulky surgical configuration made up of batteries and coils is deployed, makes from this process not the most successful one. Specifically, the batteries that got used in the past lacked a high enough energy density for powering the neuromuscular stimulators in demanding scenarios while coils for inductive coupling commonly led to misalignments or inability for powering implants located in deep tissue emplacements [7].

1.1.4. The proposed solution seeking miniaturization

Looking for alternatives, at the end of the twentieth century, addressable single-channel wireless microstimulators were proposed to be injected inside muscles in which they evoked stimulations and produced fine movements [8]. Currently, simplicity for its deployment is desired. Examples of state-of-the-art are *BION* microstimulators that had either rechargeable battery powering or inductive coupling one, this one with a reduced diameter and concomitantly, a higher degree of miniaturization. Another approach was the one of electromagnetic energy transported through propagating modes in tissue by Poon et al. [9], which had a coil diameter of 1.6 mm or even some others as ultrasounds [9]-[13], infrared light [14], [15], piezoelectric energy harvesters or physiological human electric potentials (e.g. inner ear) [16]. In this context, networks of wireless microstimulators have been issued to restore gracile gestures. As a matter of fact, their miniaturization has been a milestone that is still being developed. Here is where eAXONs prototypes enter the scene, devices developed by BERG in the past, classified as microstimulators in the active implantable medical devices (aIMDs) field. These have been meant during the current project to form a dense network to be activated by an external automated controller so that fine motion restoration was in the end achievable.

These tiny flexible implantable devices are able to locally rectify HF current bursts that go through tissues in an innocuous manner. This power transfer method is known as volume conduction or galvanic coupling and is based in the fact that the current bursts that exceed a frequency of 5 MHz, when applied in a short train stimulation, are innocuous and can elicit an electric field at the tissue level. As a matter of fact, most of the energy is dissipated due to Joule effect, but a small portion of it can be redirected to stimulate or feed an electronic deployment [17].

1.1.5. Prior validations on the proposed eAXONs technology

The history of eAXONs is relatively recent due to the time they have been present in FES scenarios since their development. However, already conducted studies integrated them in their projects. In [17] it was proposed a neuroprosthetic system in which eAXONs were to be deployed forming a dense network of microstimulators that would be individually controlled by an autonomous external unit. This unit may deliver the required innocuous HF current bursts and would individually command each microstimulator. The implantable devices should perform complex stimulation patterns in several muscles or in segments of a muscle, as those required for fine movement restoration in patients suffering from paralysis.

1.1.6. Introductory summary

As a conclusion, two main threats were encountered when performing a smooth project until reaching the ultimate goal of obtaining gracile gestures in an animal model by means of the eAXONs technology and the development of a closed-loop controller. These ones were: overcoming non-linearities arising from muscle behaviors and being able to make the most of the implantable eAXON prototypes, whose diameter was below 1 mm and allowed to obtain unprecedented miniaturized architectures in FES research projects.

All in all, these devices have already been tested to comply with safety standards (e.g. unwanted electrostimulation and tissue heating limits) as well as they have shown efficacy on in-vivo controlled charge-balanced muscle electrical stimulation, sensing skills on artificial proprioception, performing desired plantarflexion and dorsiflexion joint patterns or even grasping gestures [9].

1.2. State of the art

1.2.1. Alternatives in control of trajectories

The control of hindlimb trajectories by means of eAXONs technology and the implementation of the successful underlying closed-loop controller is the ultimate goal of the current thesis. In the past, plenty of FES closed-loop control strategies have been approached, mainly focused on plantarflexion/dorsiflexion control of ankle joints during stance phases. Some of them have been linear quadratic Gaussian, pole placement designs [18][19], H-infinity [19], artificial neural network (ANN) or sliding mode controls (SMC) [21]. Nevertheless, these ones have limitations (e.g. poor physiological basis, high computational complexity). As already stated, closed-loop is needed to accurately control the movement by receiving useful information about the system output that ultimately enters an error signal trying to fit to the specific problem requirements [22], [23]. However, their design for FES applications is a problem which still needs solutions [24]. Indeed, closed-loop control algorithms failed evoking successful performances and were not able to guarantee stability at all. Therefore, only open-loop controlled FES devices are currently integrated in clinical practices despite their limitations. Going into detail, in almost all of the tests in which the ankle was studied, it was placed in a foot pad by different ways (e.g. mechanical arm linking a servo motor). In the end, joint coordinates and motor variables have been usually recorded with potentiometers or optical encoders, depending on the problem specifications.

In this context, a compilation of some FES control strategies can be found in [25]. The open-loop performance was unsatisfactory for precise gestures control due to variations (e.g. muscle fatigue), time-variance and/or time-delay or even non-linearities. Another vast collection of techniques was focused on lower limbs [26], but few had high accuracy when applied in patients. The reason could be based in the fact that human body muscle is non-linear, volatile and its environment, complex [27]. Indeed, as already stated, entering more into the design itself of FES control systems, improving its precision is of capital relevance. Qiu et al [28] developed a PID algorithm controlling knee joint flexion and extension, but when external disturbances appeared, it was difficult to achieve the desired responses. Looking for these desired responses, a controller allowing to monitor the needed hindlimb movements was the core goal of [29] in which it was proposed a proportional-derivative (PD) and SMC for the FES applied to the musculoskeletal model of an ankle joint to track wanted gestures observed empirically on healthy patients during gait cycle. Following the point of this SMC, it is one of the golden choices when it comes to dealing with effectiveness on non-linear robust controllers, since it facilitates conditions by matching system dynamics uncertainties with disturbances. As an example, in [30] a fuzzy sliding mode controller was postulated, the one that corrected external errors. Another conducted experiments have made use of closed-loop controllers as well, such as [31], where they combined a motor and a FES control system that allowed the patient to ride with a certain sustained cadence. In [32] a pioneer closed-loop control approach of muscle stimulation to rehabilitate reach-to-grasp maneuvers following stroke and spinal cord injury was approached.

All in all, every single developed controller designed to accomplish desired gestures in an animal's hindlimb has been mostly designed MATLAB Simulink tool, in which certain saturation blocks were included as well in order to limit the extent of the FES amplitudes given to the subject (20 - 60 mA for plantarflexors and 20 - 45 mA for dorsiflexors) [33]. Fatigue, spasticity or gravity are other factors that could potentially distort plant's performance. Extensions such as integral and velocity blocks can make it to PIV and integrate dynamic joint-angle feedback, even adding anti-windup strategies. These extensions can make the results be as close as possible to the desired ones, since in [34] they eventually evoked smooth eccentric motions and sinusoidal gestures with low time delays. Other movement control strategies have been performed, such as a multiple-input single-output (MISO) real-time closed-loop plant to assess asynchronous intrafascicular multi-electrode stimulation (AIFMs) to process precise, fatigue-resistant and isometric muscle twitches in anesthetized felines [35] or a set of gyroscopes guided arm maneuvers and used a non-linear controller, the robust integral of the sign of the error (RISE), to evaluate the capability of controlling FES in closed-loop [34]. Another example to bear in mind is [36] in which a PI plant modulated the pulse width of a train of fixed-amplitude stimulus which evoked activations in the medial gastrocnemius (it estimated the error between target joint angle and the expected joint coordinate).

More complicated algorithms have been done, such as the closed-loop functional optogenetic stimulation (CL-FOS) system to control ankle joint positions in murine models [37]. All in all, among already constructed feedback controllers, fuzzy logic ones (FLC) have shown proper control performance when handling complex non-linear systems. Recalling the initial statement, the open-loop performance was poor for accurate movement control in [38][39][40] since this option was not able to assess the required muscle stimulation intensity to elicit the needed angle for a certain limb's movement [39]. Apart from that, remarkable is the fact that 4 to 8 multichannel electrodes are needed to perform a successful hindlimb movement control and account for smooth muscle spasms [41][42][43]. Therefore, as a conclusion, while plenty of open-loop solutions have been deployed in the past, scarce ones are found as closed-loop architectures.

Indeed, the accomplishment of a successful controller allowing precise gestures with a single degree of freedom is still a concern in the FES field and one of the main lines of study.

1.2.2. Modeling and simulation approaches

Once the alternatives in control of trajectories were understood, the next step was to count with the modeling tools of a FES system under study, the ones that have empowered the designs of AIMDs pursuing certain animal or human movements (e.g. grasping) in paralytic individuals [10]. In this context, disposing of a musculoskeletal model in which one could assess the dynamics that may happen once certain forces, strengths, loads and external perturbations were applied, has accelerated and enhanced the results of projects in the field.

In this context, it was decided to go with OpenSim, a software, with licenses under Open Source basis, which performs the computations of variables from a musculoskeletal model that naturally may be calculated empirically (e.g. muscle evoked forces, tendon stretchings). Apart from that, it offers the possibility to make predictions on novel gestures. In the past, some OpenSim research when it comes to rat hindlimb studies in FES or similar anatomic ones has been developed. In [47] the Static Optimization (SO) tool used the minimization of sum-squared excitations as cost function, but as this tool considers individually each frame in time, SO is discarded for the present project in detriment of a Forward Dynamics simulation. In [48] a FD simulation follows a residual reduction algorithm (RRA) that refines the OpenSim model kinematics so that they are more dynamically consistent with the experimental reaction forces and moments. In [49] a musculoskeletal simulation analysis was performed so that a preoperative FD simulation performing a stair descent scheme was constructed. In [50], the integration of the MATLAB interface to the OpenSim API develops a framework for solving this kind of musculoskeletal optimal control problems, combining the programming, design and control abilities of Simulink with OpenSim musculoskeletal modeling, simulation and assessments. All in all, OpenSim, despite not being valid as a thesis result, will serve as basis and future lead of research given its powerful capabilities of new time frames computations.

1.3. Hypothesis and objectives

1.3.1. Core hypothesis

In the present study, the core hypothesis is the one that stands for the ability to accomplish gracile movements control with presumably 1 degree of freedom (DOF) in agonist / antagonist muscle pairs, making use of the eAXONs technology. Remarkably, until the date, at least in Open Source literature, no study has been able to obtain those DOFs in animals.

1.3.2. Primary objective: Control the position of the feet

The most ambitious part of the project under consideration is accomplishing the movement control with 2 DOFs by means of muscular stimulation performed by eAXONs Technology and settle down the basis for future accomplishment of fancy gestures, such as circular or sinusoidal trajectories.

1.3.3. Secondary objective

1.3.3.1. OpenSim lead: Musculoskeletal in-silico model construction

The construction and preconditioning of a 3D musculoskeletal rabbit model allowing to predict dynamical parameters (e.g. angles, coordinates, angular velocities, accelerations) thanks to electrical stimulation applied forces was considered as an interesting lead of development.

Being conscious about the possibility to count with a rabbit musculoskeletal model that may help understand better the dynamical implications of stimulating certain muscles from its anatomy, the first step was choosing an already preconstructed model from the literature that allowed to save time when it came to designing one from zero. However, this secondary objective, given its difficulty on the technical Deployment, has not been successful and operative, but may serves as reference for further investigations in the field.

2. Methods

Three experimental sessions were conducted at CMCIB with New Zealand male white rabbits weighing approximately 5 kg. Seeking for a proper control of the feet position, a 3D-printed platform allowing for the immobilization of the animals' hindlimb was constructed. Apart from that, two muscles were the ones in which implanted procedure was conducted: TA and MG.

On the one hand, TA accounted for dorsiflexion gesture. An electrode was injected in the thigh of the vertebrate, thanks to a 10M Electrode Hook Wire that guided the implantation. The implantation itself followed some rigid criteria: it needed to be performed 3 cm inside the muscle and arrive to the final of the conduct. Before conducting the experiment, two current trials were performed in order to appreciate the muscular response. A current threshold for the implant to elicit a dorsiflexion movement caused by the TA was annotated. Besides, the feet returned to the origin position when the current burst ended. MG accounted for the plantarflexion, and its muscular surface was larger than the one from TA. Besides, as commented, the heterogeneity of the muscular spindles made expectable the fact of observing afterwards ripples in the signal coming from the muscular response. In the case of MG, the implantations needed to be superficial since if not, the entry could be confused with the soleus. Apart from that, the incisions performed by the interventionist were performed 0.5 cm away the lateral gastrocnemius in order to avoid latter artifacts in muscular stimulations.

2.1. The aim of the preliminary assays

The conducted preliminary assays were aimed to experimentally validate the initial hypothesis: to demonstrate that precise hindlimb movements with 1 DOF in agonist/antagonist muscle pairs can be obtained by means of the development of a closed-loop control making use of the eAXONs technology. The reason of these eAXONs use is based on, as already commented, the urgent need in the field to perform an enhancement of implantable FES architectures with respect to their miniaturization of its still bulky configurations. This reduction towards the minimum sizes would strongly reduce the injuries and difficulties when deploying the system percutaneously as well as would help recruiting muscle fibers in a wider and better way. This is where eAXON prototypes shed light to. As a general fact, the architecture for this kind of addressable single-channel wireless microstimulators deployed by injection procedure usually follows a general flowchart, considered as the gold-standard: in principle, these microstimulators are to be forming a dense network powered by an external controller that works in an automated way, pursuing soft and fine movement restorations.

In this context, the used eAXONs thanks to its advantage of diameter sizes with respect to their homologues, allow them to be selective in terms of stimulation locations. These devices can, once the whole system has rectified epidermically applied high frequency (HF) current bursts, elicit muscular action that in the end, can be controlled by means of an algorithmic scheme. All in all, unique target stimulation is not enough to elicit a successful movement restoration when the subject under study is paralytic. Therefore, the main reason for deploying a dense network of eAXONs is this one; count with many actors performing target stimulations that are proper to do their best when restoring lost muscular gestures. These all are to be controlled by the autonomous external unit, the one that delivers innocuous HF current pulses and commands uniquely each eAXON.

2.2. Animal preparation

Having taken into account the goal of the trials, it was time to go with their preparation. Here, since animals were involved, an approval coming from a local Ethical Committee was needed to conduct the in vivo sessions at the CMCIB Barcelona, in which two experimental assays were performed with two different adult male New Zealand rabbits, one per day, weighing 4.3 - 4.6 kg.

The rabbits got anesthetized by intramuscularly applying drugs. Before conducting any kind of incision, the left hindlimb of the rabbit got shaved from the head of the femur to the tip of the tarsus bone. Then, the animal was intubated during the whole experiments and monitored thanks to a pulse oximetry and capnography. A heating pad located at the surface of the surgical table kept the bodily temperature inside safe margins (36.3^{o} C - 38.6^{o} C). Having finished each of the sessions, the animal was applied an overdose of a euthanizing drug.

2.3. Implanting procedure

Once the animal protocol was validated and the session was ready to be approached, it was of the utmost importance to have clear the implanting procedure of the eAXONs in the rabbit's hindlimb. For the preliminary assays, two muscles were the final choice to proceed with the implantation scheme: TA and MG. The implantations on both muscles were focused on their respective motor points (muscular location in which the excitability reaches its peak). The main reason for which MG was chosen is no other but the vastly known intramuscular innervation behavior as well as the facilities when accessing nerves in the boundaries and the heterogeneous nature of the fiber types. Since this heterogeneity may lead to different activation patterns, one may expect more fluctuations and ripples if compared with the other muscle under study, TA.

For the experimental sessions conducted in vivo, the eAXON prototypes were tested percutaneously (thanks to a bipolar flexible probe) with the previous introduction of a hook wire until a muscular deepness of 10 mm all the way parallel to the nerve. Initially, an intravenous catheter was longitudinally injected from a location close to the TA muscle. A custom-made generator performed electrical stimulations. Once the proper motor point was found, the introducer needle got removed. An identical flowchart was done to find the motor point of the GA. In the end, catheters were withdrawn and probes fixed to the skin. Each of these probes was intertwined to one circuit prototype.

The final aim to elicit muscular movements whose error led to the chance to control trajectories by means of a Simulink controller.
Dorsiflexion and plantarflexion joint movements were performed and controlled.

2.4. The electronic system and how the stimulation is applied

Once the procurement of certain muscular movements was planned, it was time to study the architecture of the electronic System under use, as well as the flowchart of the stimulation. Here, it was necessary to count with an external system formed by three main blocks listed below:

- A computer generating the modulating signal
  In order to send the needed bursts to the animal's muscles, it was needed to count with the proper electronic architecture.

- A carrier generator and modulator
  In this context, a card incorporating a microcontroller from STM32 family sent via USB commands which activated an analogic signal (ranging 0-5V) and connected to the function generator which, in turn, used as modulator ASK (Amplitude Shift Keying) in order to properly activate or deactivate the HF sinusoidal signal (6.78 MHz).

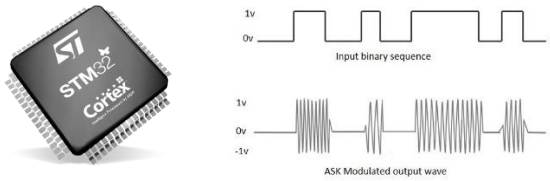

Figs. 1, 2: Microcontroller from STM32 family (left) and Amplitude Shift Keying method (right)

The microcontroller itself already had on it the basic parameters accounting for the required burst to activate the implants. Besides, the possibility to modify those parameters was given thanks to the commands to be given via USB.

- A high voltage amplifier
  The output of the generator was connected to an amplification stage specifically conceived for the current assays, having an approximate gain of 30 (dimensionless).

The generated signal was delivered across a pair of 3 cm wide band electrodes made from silver based stretchable conductive fabric strapped around the rabbit's hindlimb where the bipolar probes were implanted.These prototypes are defined by some key features:

- A demodulator for the amplitude modulation (AM) communications system.
- A power supply unit.
- A digital control system (microcontroller).
- Two current sources generating biphasic currents.
- A Schmitt trigger for waking up digital control unit when a HF burst was sensed.

2.5. 3D printed pieces

Having arrived to the point in which the aim of the experimental sessions was clear, the protocol for the animal handling approved, the implantation scheme was infal·lible in terms of detailed descriptions and the stimulation flowchart completely defined, it was time to go with the deployment of a mechanical exoskeleton printed in 3D pieces, aiming to immobilize the hindlimb of the rabbit in a sideways manner. The 3D-printed exoskeleton design was necessary to account for 1 DOF in the agonist / antagonist muscle pair of TA / MG, allowing to neglect gravitational effects since the hindlimb was placed sideways and its movement restricted to the desired one. Fusion 360 by Autodesk allowed to design the apparatus accounting for this. In this scenario, the final goal was to obtain a .STL file which could be directed to its 3D printing.
This Computer Aided Design (CAD) ultimate architecture was followed by a designing iteration that is shown below. In the end, two solid finite elements formed the final model. As a matter of fact, the final tibia 3D-printed piece is from Marc Tudela's contribution.

Initial idea:
Originally, 3 pieces (femur, tibia, feet) formed the model. However, due to large amounts of friction when the elements got intertwined between them, forced the design to be iterated until arriving to a final one integrating the key elements to be explained afterwards (encoder, screws, bearings).

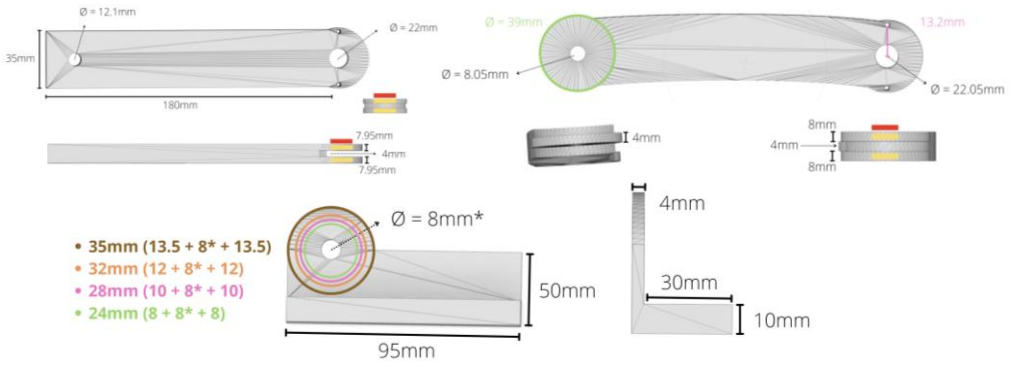

Fig. 3: Sketches from the 3D initial idea printing designed with Autodesk Fusion360

Final design:

In the end two main elements made up the whole architecture. These are listed below. Since all of them are similar in construction, the design procedure can be generalized to:

- Do the initial sketch in order to extrude the needed volume afterward.
- Position holes through encoders pass (a tolerance margin was added)
- Design holes for the straps using the pattern tool.
- Finish for each joint so that they can be integrated with negative extrusion.

FEMUR

Front side	15° side	Lateral side	General view
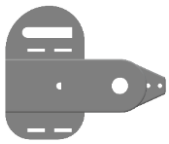		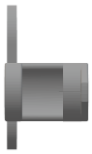	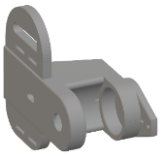

Figs. 4, 5, 6, 7: Different views from the 3D-printed femur

TIBIA AND FEET

Front side	15° side	Lateral side	Upper view
	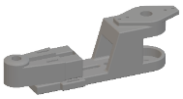		

Figs. 8, 9, 10, 11: Different views from the 3D-printed tibia and feet

All in all, below the whole designed mechanical set-up can be glanced:

Upper view	Lateral view
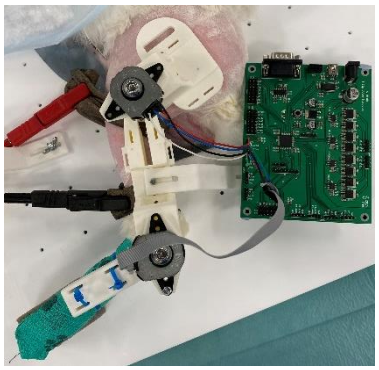	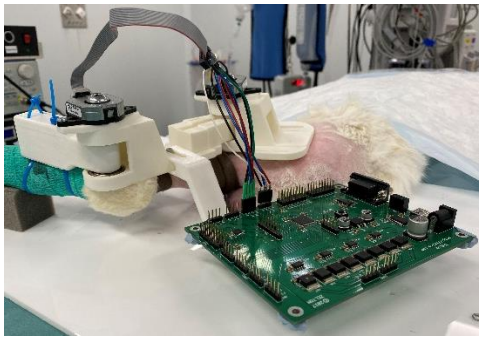

Figs. 12, 13: Upper and lateral views of the whole system integrating the elements described in this section

2.6. Simulink closed-loop controller

As a final step before integrating all the methods in one and begin validating the assay set-up in the surgical room, it was of the utmost importance to avoid stationary errors and accomplish a precise and smooth response. This precise response is not straightfoward, and indeed, muscle dynamics is usually defined by some uncertain non-linearities as well as input delays. These phenomenona make capital the fact of disposing of a closed-loop plant in FES scenarios that may help control the movements that are produced by the HF bursts in the animal's hindlimb and ultimately, track the desired trajectories [51][52][53]. This is the goal of a Simulink closed-loop control: to be sovereign on the muscular trajectories performed by the rabbit and, in the end, demonstrate the possibility to obtain certain gracile gestures.

A closed-loop control applied in a FES assay allows to enhance the stability, reduce outer perturbations and make the most of the system's precision [54][55][56]. Here, thanks to the feedback arising from the encoder recording coming from each of the articulations, an error signal determines the level of modulation needed to correct the trajectory and make it fit the desired ranges. This process is the so-called uplink communication, where the interface between an external system and the injected microstimulators is put in common [57]. Following the point of a stability improvement and muscle fatigue reduction, the feedback is crucial, which switches on and off the current bursts and, concomitantly, the stimulations, when needed [58]. In the past, closed-loop controllers were directed mostly to assess ankle joint in plantarflexion/dorsiflexion stance phases.
Studies include pole placement designs [59], artificial neural networks [21], sliding mode controls [60] or even linear quadratic Gaussian [61][62] and pole placements [63], among the ones common drawbacks appear, such as those of concerning computational complexities or scarce physiological-silico correlations.

What it does with the controller itself, it was decided to go with a PID one to conduct the experiments. A flowchart of dorsiflexion and plantarflexion movements was discriminated inside the controller so that its parameters could be discerned, fitting them the best possible for the trajectories control. Therefore, the closed-loop controlled FES got bilaterally implemented in the ankle plantarflexors and dorsiflexors, ultimately generating an error signal that got as input to each of the two PIDs, with derivative term neglected (D = 0) whose formulas were defined as follows:

$$P + I \cdot T_s \cdot \frac{1}{z-1} + D \cdot \frac{N}{1 + N \cdot T_s \cdot \frac{1}{z-1}}$$

A derivative filter gain could have been added as well to study the possibility to reduce HF noise amplification. Besides, as a future lead, it is worth to assess the fact of adding nonlinear blocks to the muscles and the model when huge loads or variations are to be applied, since they could be helpful in improving the accuracy of the closed-loop controller [64]. Aiming to specify these rabbit-specific PID plant parameters, several trials were performed, including ramps, sinusoids and constant signals. The success on the closed-loop controller performance is defined by the way the output is stabilized once the input has entered the system. As a matter of fact, extremely low sampling frequencies made the system tend to have large inaccuracies, ultimately receiving faulty encoder readings. Besides, the friction when the hindlimb was being displaced at the top of the platform surface was very low, making the incipient peaks of the response to be extremely sudden, aggressive and deep. The corrent controller was designed by Marc Tudela.

Once taken this into account, animal fatigue was another concern that may paralyze in certain moments the assays due to the absence of muscular response. Seeking for a solution, it was decided to randomize the trials order as well as to wait around 45 seconds between concatenated stimulations. One of the objectives was to tune the PID parameters and to make them as individual-specific as possible. This was accomplished considering each of the muscular responses among the different rabbits used in the preliminary assays. However, as a general tendency, and seeking for reproducibility in the studies and briefness in the numbers, PID parameters from one of the sessions were considered as gold standard, and in the rest of sessions, little modifications were applied to them. A visual reference was marked in the basement of the mechanical platform in order to begin in the same position in every single response. Most of the times, the experiments began in the 0^{o} offset marked position; however, others were intentionally initialized in other positions (e.g. -10^{o} in dorsiflexion gestures). The step function of 5 seconds served as the evaluator for the initial offset position. Knowing there were 2 PIDs accounting for a different hindlimb flexor movement, each of them needed to get defined the different controller parameters. In both, integral was given always the highest absolute value, ensuring that the steady-state error stood close to zero. However, even though integral term is useful to minimize the steady-state error, it can produce as well huge overshoots in the response as windup cause (this phenomenon happens when the desired response follows sudden changes, and its error integral accumulates when the response is on its rising stage). Derivative was set to 0 always. Apart from that, smooth increases to the proportional term led to stable and fast transient responses, ending up in underdamped conditions.

All in all, and before conducting any kind of trial, the dynamical response of plantarflexors and dorsiflexors to different bursts amplitudes was assessed, having the animal placed sideways, fixed to the mechanical platform and allowing for 1 DOF. Trains of FES pulses were sent at a constant frequency (50 Hz), different durations (around 50 ms, 100 ms) and burst amplitudes (varied from 50 to 200 mA). Interestingly, the ramp pulse leaded the system to show some hysteresis, since apart from the static damping, some dynamical friction arose, making the index to be different than that of the angular encoder reading. The saturation of the controller was ignored when the system was being linearized. Finally, the anti-windup strategy was based on the clamping method in all cases. In the controller output, saturation blocks were to be added aiming to restrict the ranges of current amplitudes (generally 200 and 35 in for upper and lower limits respectively for dorsiflexors, 200 and 5 for plantarflexors). The threshold for current amplitude to fall upon 0 mA was 2 mA. Peak-to-peak (pp) voltage responses ranged 121-125 Vpp and what it did with the currents, 384-388 mA pp. Frequencies below 30 Hz were producing tetanizing gestures, or what is the same, muscular responses in which the needed summation of spindles was not reached to be self to produce a proper complete muscular flexion. Scopes at the outputs of certain merge blocks allowed to visualize the status of the stimulation in contrasted timeframes. In the end, an ASCII writing was coded and ultimately interpreted by Simlab. As a nuance to take into account, the region in which the TA and MG overlapped responses was extremely short (approximately 15-20% of the total goniometric circumference defining the path). Automatic fine-tuning of the PID parameters was not approached in any case.

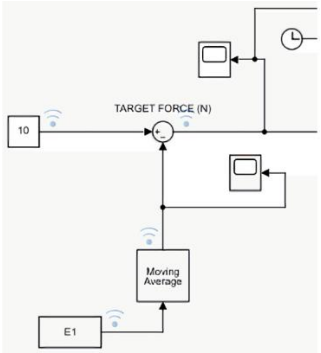

Here, the input of the encoder recording is fed to a moving average block, the one that computes the moving average of the input signal along each channel independently over time.

Once this has been processed, a scope allowed to glance it. All in all, the error signal arises thanks to the comparison of the reference input, in this case 10, and the one measured experimentally and coming from the moving average block's output.

Fig. 14: First module of the SIMULINK controller

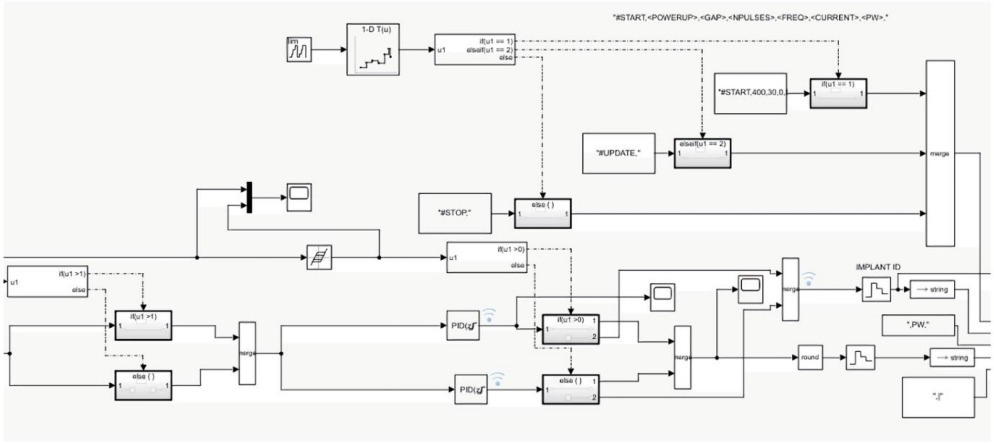

Fig. 15: Second module of the SIMULINK controller

Above, the error signal coming from the previous comparison between reference and measured angles, enters a conditional in which if the error is positive, goes to one side, and elsewhere, to the other, ultimately leading to the same destiny: a merge block that allows to continue the flowchart upon arriving to the PID (D=0) controllers themselves, the ones that were activating whether one implant or another depending on the sign of the signal. As a matter of fact, pursuing to have some hysteresis in the system that may allow having a reduced switch-like behavior, extremely digital, the one that was leading to the activation of one implant or another, two draft proposals were posed, being the last the chosen one:

1) Implement a conditional block at the output of the error signal that, when a certain angular threshold was reached, gave an error of 0, and elsewhere, the real error.

2) Apply a backlash MATLAB block, where an input variation leads to the same modification in the output. However, when the input changes sense, the offset input variation does not play a role on the output. Here, deadband accounts for the side-to-side span range where its center is located around the output.

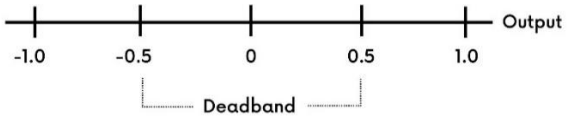

Fig. 16: Infography summarizing the functioning of the Backlash MATLAB block

Once taken this into account, a set of listed parameters defining initialization times, stops, applied currents as well as their amplitudes, number of pulses and frequencies, blocks of start and update of status were added so that in the end, the command was to be sent to the board and converted to ASCII format in order to be readable and interpretable for it. Below, the final delivery to the communications port once all the translation process was accomplished.

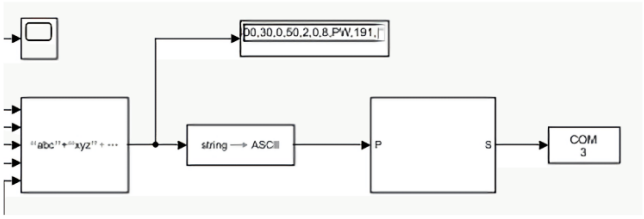

Fig. 17: Third module of the SIMULINK controller

2.7. Used elements for the set-up building

Last but not least, when all the session was planned, it was needed to embody in the 3D exoskeleton the necessary pieces and elements accounting for the desired gestures control. This was the very last step inmediately before applying the stimulations.

OPTICAL ENCODERS

An AMT20 modular absolute encoder by CUI Devices was implemented in each of the joints under study (ankle, knee). These low power consumption and compact items allowed to record the angular movements and deviations performed by the animal's hindlimb once the applied bursts overcame the needed threshold to elicit muscular action. Some of the key features are listed below:

- ELECTRICAL
  - Power supply: 4.5 – 5.5 V
  - Start-up time: 200 ms
  - Current consumption: 8 – 10 mA
  - Output high level: VDD – 0.8 V
  - Output low level: 0.4 V
  - Output current: 2 mA
  - Rise / fall time: 30 ns
- INCREMENTAL CHARACTERISTICS
  - Channels: Quadrature A, B and Z index
  - Waveform: CMOS voltage square wave
  - Phase difference: A leads B for counterclockwise rotation, 90º
  - Quadrature resolutions: 96, 192, 200, 250, 384,…, 500, 512, 768, 800, 1000, 1024
  - Index: One pulse per 360º rotation
  - Accuracy: 0.2º
  - Quadrature duty cycle: 50%

Once integrated into the 3D-printed architecture, a basic Simulink diagram was tested in order to assess whether quadrature inputs were successfully connected to the board, as well as the angular recording was being smooth and as expected.

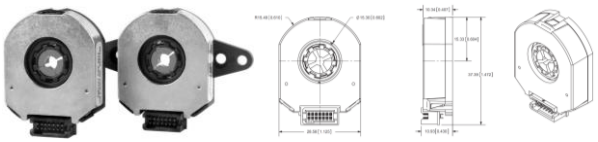

Fig. 18: Used modular absolute optical encoders belonging to CUI Devices (AMT20)

SCREWS, STRAPS

Seeking for a proper animal fixation, some screws at the level of the knee and wrappings around the animal's hindlimb were placed so that the desired 1-DOF were the single allowed one.

TEXTILE TROUSERS

Aiming to have the surface textile electrodes as tight as possible to the animal, in the last experimental session, textile trousers got manufactured so that a comparison between a session without them and another with them being used could be hypothesized.

Fig. 19: Textile trousers made from lycra in-house

BEARINGS

A set of 8mm-inner diameter LUIJZZ 608 ZZ bearings was acquired to allow for a smoother rotation of the encoder axis when the interfaces among joints were sliding. Holes in the 3D-printed model were performed so that they could be inserted inside.

Fig. 20: Dimensions schematics of the used bearings belonging to the LUIJZZ 608 ZZ family

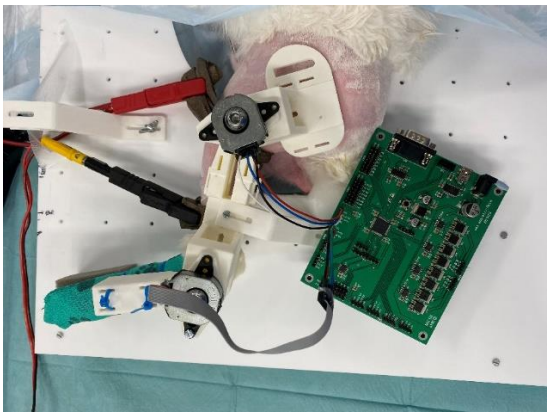

Fig. 21: Schematics of the whole set-up in an upper view

3. Results

In Functional Electrical Stimulation, the achievement of simplicity when deploying microdevices that previously were as much miniaturized as possible, is the core goal. Following this point, the electrical rectification of innocuous HF current pulses applied in tissues through these implanted eAXONs, allows to locally stimulate regions of interest. Known this, the present thesis aimed to modulate the muscular response at first and, secondly, apply a closed-loop plant that made possible to correct undesired trajectories errors and conceive controlled gestures of the rabbit's hindlimb. These corrections were mainly based on information coming from joint angles feedback (encoders recordings located at the articulations of the ankle and the knee). Apart from that, other studies in the past considered other variables such as myoelectric activity, pressure behaviors or magnetic field goniometry. This all may lead to an ultimate controlled and natural hindlimb trajectory. Therefore, it has been validated the objective of demonstrating the possibility to electrically rectify pulses applied by addressable microstimulators and, ultimately, control the angular trajectories they elicit thanks to a closed-loop controller designed with SIMULINK.

Seeking for simplicity in the results report, the first two conducted experimental sessions are described below. On the one hand, the first was conducted under closed-loop and open loop architectures in order to make comparisons and extrapolations in terms of hindlimb trajectories once the stimulations were applied. On the other hand, the second experimental assay was purely conducted under a closed-loop architecture, aiming to validate results from the preceding session and demonstrate a kind of inter-trials reproducibility.

3.1. Session 1: Closed Loop architecture with a 50 Hz stimulation frequency

In the first experimental session conducted with a New Zealand rabbit weighing 4.2 kg, Tibialis Anterior (TA) was the chosen target muscle. The applied stimulation frequency was of 50 Hz, which means that was half the one used in Open Loop trials (100 Hz).

Even though, originally at the beginning of Closed Loop experiment the programmed frequency was of 100 Hz, amount that fatigued excessively the animal and it was empirically decided to reduce it until half the initial one. As a matter of fact, it is not recommendable to go varying frequency in trials in which fixed conclusions and reproducibility are chased. Four different trials were conducted, in which, beginning from an offset position (0^o) marked in the platform in which the animal was laying sideways, certain angle ranges were specified to be followed by the hindlimb. An encoder placed in the animal's ankle recorded the performed trajectories that afterwards were displayed in a plot representing them in angles (^{o}, "Encoder input") during a certain period.

	Encoder input	PID Controller
5º	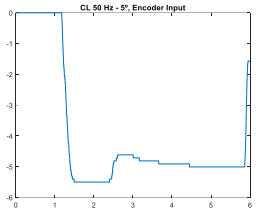	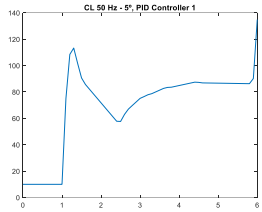
10º	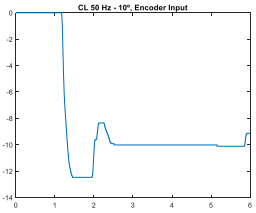	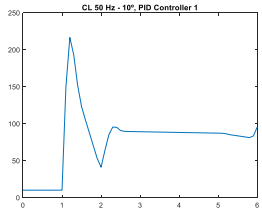
15º	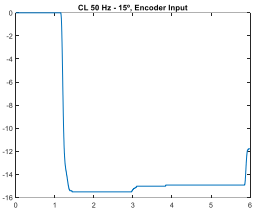	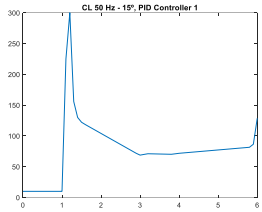
Ramp 0º/10º	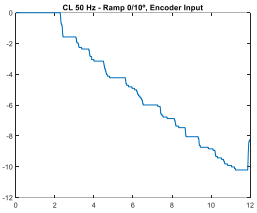	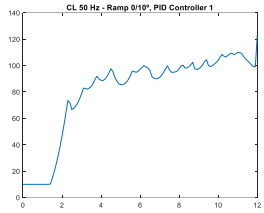

Table 1: Collected graphs about encoder inputs and PID controller during session 1 in CL architecture

Apart from that, a Simulink controller integrated two symmetric PID plants (explained in the corresponding section) accounting for the places in which the implants had been previously injected. Since in this session just TA was the target location in which implant got injected, only a single PID Controller was being operative in the said TA muscle. Above, in controller graphs, horizontal axis (OX) was in time units (seconds) and the vertical one (OY) referred to stimulation burst duration (μs).

	Rise time (s)	Overshoot (μs)	Peak time (s)	Settling time (s)
5º	0,172	-5,497	1,848	4,29
10º	0,11	-12,468	1,677	2,518
15º	0,105	-	-	2,309
Ramp 0º/10º	7,818	-	-	11,207

Table 2: Summary of dynamical parameters during session 1 in CL architecture

3.2. Session 1: Open Loop architecture with a 100 Hz stimulation frequency

When it came to applying the same experimental flowchart, this time with no error correction mechanism, three new trials with contrasted stimulation burst durations (100 μs, 150 μs, 250 μs) were performed. Same process for the encoder input recording was applied.

As a matter of fact, PID Controller plots are included in order to demonstrate the flat tendency of them, with a horizontal line located at the vertical height that the applied stimulation burst duration indicated (100 μs, 150 μs, 250 μs).

	100 μs	150 μs	250 μs
Encoder input	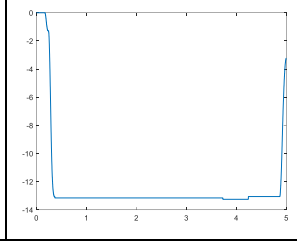	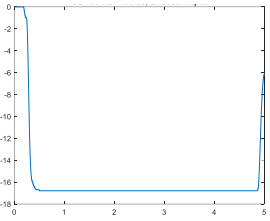	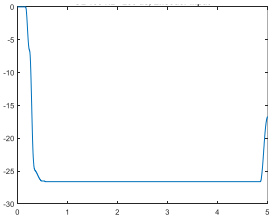

Table 3: Collected graphs about encoder inputs during session 1 in OL architecture

3.3. Session 2: Closed Loop architecture with 100 Hz stimulation frequency in TA, MG.

In the second experimental session conducted with a New Zealand rabbit weighing 4.5 kg, Tibialis Anterior (TA) and Medial Gastrocnemius (MG) were the muscles under study. The applied stimulation frequency was of 100 Hz.

Seven different trials were conducted, among the ones three (-10º, 10º, ramp) were performed under a dynamical friction arising from a foam located in the interface between the feet and the basement (in muffled conditions, this allowed to be able to add a dynamical load to the displacement and assess the consequences in terms of controller dynamics). This time, since implants got introduced in both locations (TA, MG), 2 PID Controllers were assessed, each accounting for a different muscle.

	Encoder input	PID Tibialis Anterior	PID Medial Gastrocnemius
-10º normal conditions	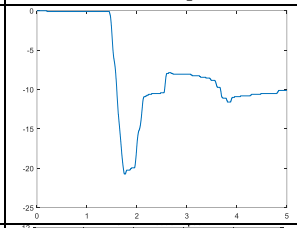	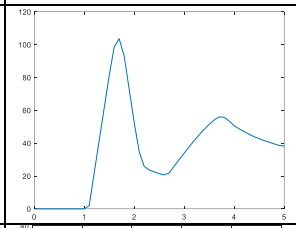	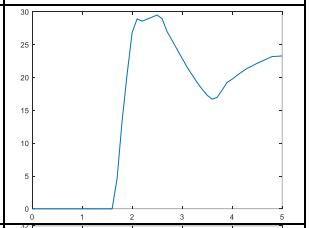
10º normal conditions	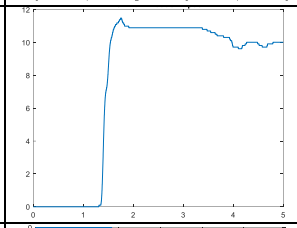	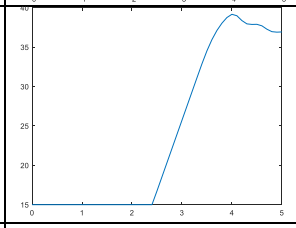	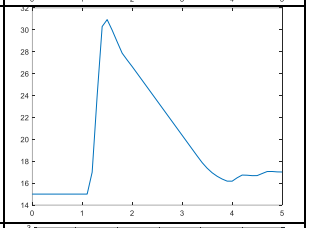
- 10ºmuffle	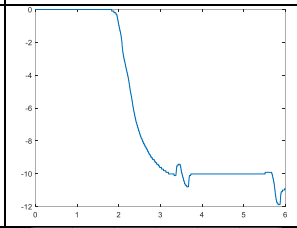	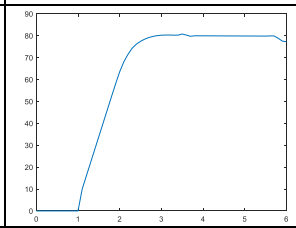	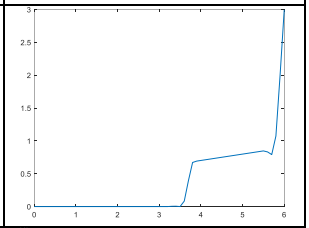
10ºmuffle	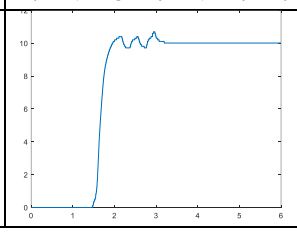	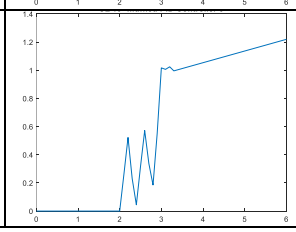	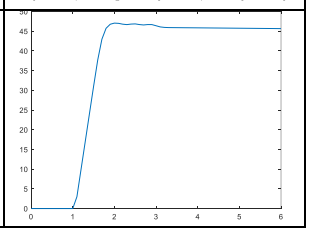

Ramp muffle	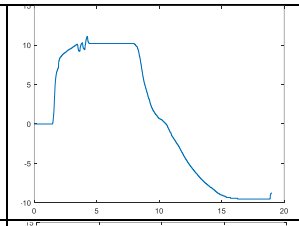	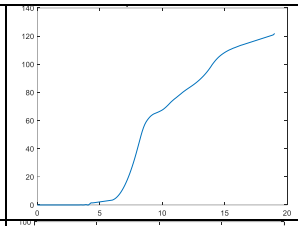	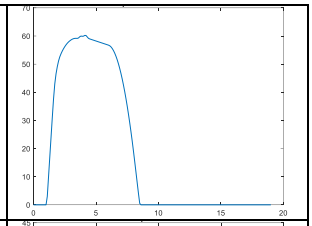
Sweep 10º / - 10º	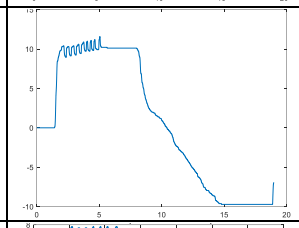	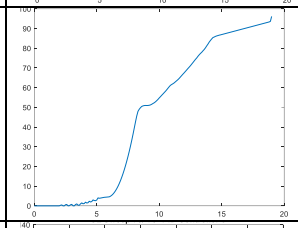	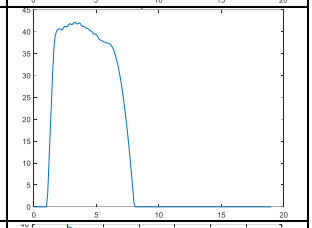
Sweep 75º / - 75º	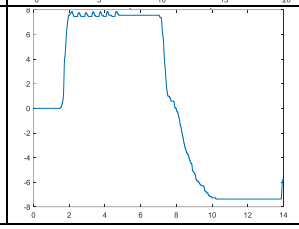	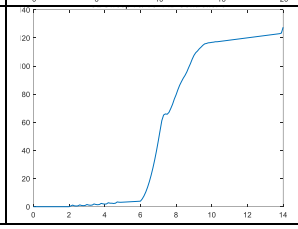	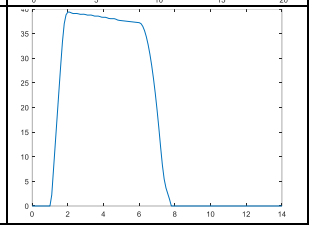

Table 4: Collected graphs about encoder inputs and PID controllers during session 2 in CL architecture

Criteria to bear in mind when extrapolating conclusions on the controller performance are the following, the ones that can be glanced in the image below, representing the trial conducted in the second experimental session in a Closed-Loop architecture, ramp reference input and a goal of -10º.

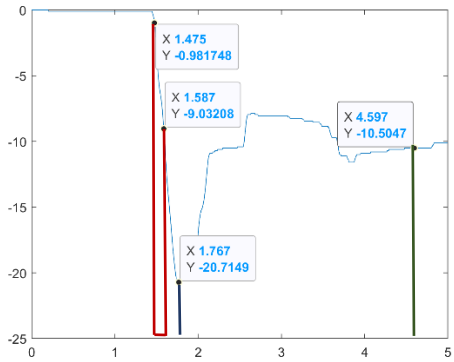

Fig. 22: Infography of way the dynamical parameters get extracted

- Rise time (T_r) is the time it takes the response to go from 10 to 90% of steady state
- Settling time (T_s) is the time it takes response to settle within ±5% of steady state
- Peak overshoot time (T_p) is the time it takes response to reach first peak overshoot

	Rise time (s)	Overshoot (µs)	Peak time (s)	Settling time (s)
-10º	0,112	-20,71	1,767	4,597
10º	0,138	11,49	1,751	3,671
Sweep 10º/-10º	0,272	10,31 (1st one)	2,109 (1st one)	14,547
Sweep 75º/-75º	0,27	7,76 (1st one)	2,118 (1st one)	10,296

Table 5: Summary of dynamical parameters during session 2 in CL architecture and normal conditions

	Rise time (s)	Overshoot (µs)	Peak time (s)	Settling time (s)
-10º muffle	0,802	-10,01 (1st one)	3,33	4
10º muffle	0,253	10,41 (1st one)	2,156	3,097
Ramp 10º/-10º muffle	0,938	10,11 (1st one)	3,394	15,33

Table 6: Summary of dynamical parameters during session 2 in CL architecture and muffle conditions

4. DISCUSSION

The background

Having presented the results of the two conducted experimental sessions, it has been demonstrated that certain successful trackings of desired angular steps, ramps, and sweeps under different friction scenarios in the mechanical platform sustaining the rabbit have been accomplished thanks to the information given by a real-time joint-angle feedback recorded by optical encoders and controlled by means of a closed-loop plant. This deployed controller had a variable functioning over time, so the lack of non-linear behaviors made the designed plant not to count with a transfer function. Technically, since the said transfer function was not known, the approach was based in *ad-hoc* decisions.

The friction

Having clear the background, it was time to get hands to work technically speaking, and once the whole stimulation architecture was ready in the first session to obtain the incipient results, it was seen that the constructed mechanical exoskeleton allowed excessive movement freedom, arising from the lack of loads in the hindlimb that may complicate the sliding of the rabbit's leg over the basement's surface. This led to huge and extremely sudden overshoots in the encoder readings, aspect that was taken into account for the second experimental session. This problem of an excessive overshoot in the response led to think of a solution consisting of placing a foam between the platform's surface where the hindlimb was laying sideways and the leg itself. This set-up accounted for scenarios with different degrees of friction (underdamped without foam placed in the platform, and overdamped with the foam on it). All in all, in nature, a classification of three different damped conditions is ruled by:

- **Underdamped**: the damping ratio is $0<\zeta<1$. This is the most common case and the only one that yields oscillation. Most of systems found in physical world vibrate like this.

- **Overdamped**: Ratio is $\zeta>1$. It does not oscillate and it returns to its rest position exponentially being also slower to respond than a critically damped system.

- **Critically Damped:** Value of damping ratio is $\zeta=1$, no oscillation occurs. It has the value of damping providing the fastest return to time zero without oscillations.

The closed-loop architectures

Having clear the location of the optical encoders, the angular excursion of the hindlimb was what was being analyzed, and when trying to follow 5^o, 10^o and 15^o in non-friction scenarios was almost identical in terms of rising (0.172 s, 0.11 s, 0.105 s) and settling times (4.29 s, 2.518 s, 2.309 s), while when a certain foam located between the platform and the leg was placed in the second session, under the same conditions, the overshoot dropped from -20.71 μs to -10.01 μs for the excursion of -10^o tracking and from 11.49 μs to 10.41 μs for the 10^o tracking. Besides, the settling times were reached way before, arriving to the final steady-state earlier (4.597 s for the -10^o in normal conditions compared to 4 s in the -10^o muffled scenario). In the end, a slight increase in angular position noticiable in all the plots means that tendon influence on the hindlimb tried to counterbalance the offset position of the leg, the one that as already stated, began in a 0^o offset position. Apart from that, as it was expectable, the ramp had the slowest temporal behavior, mainly caused by the dynamic friction that the excursion presented, apart from the static one that, despite being small, was present during all the trials.

Among the aforementioned three friction classifications, the second experimental session took into account two of them. In this context, and just before entering into the discussion of the purest results, it is worth to bear in mind that one of the major limitations in the FES field nowadays is the inability to obtain gradual muscle forces and ultimately, smooth trajectories, since the fibers from most living organisms have an on/off nature. Besides, the rapid muscle fatigue that is produced in them due to the large stimulation frequencies needed to evoke the desired gestures as well as the opposite recruitment of fibers (fast-fatiguing fibers are activated before slow-fatiguing ones) adds even more complexity to the tracking of these desired hindlimb gestures. Recalling the friction classification, in the second session four underdamped trials were conducted (-10º, 10º, sweep from 10º to -10º and sweep from 75º to -75º) as well as three overdamped ones (-10º, 10º, ramp from 10º to -10º). Here, rising times for the overdamped trials were 2-5 times larger than the ones in underdamped, since oscillations of the underdamped led to earlier and larger overshoots.

Large initial overshoots, most of the times, are cause of large Kp constants of the controller. In this case, rise and peak times were almost identical in the -10º and 10º underdamped cases, as well as their respective settling times. However, -10º led to a much larger overshoot. Apart from that, the obtained sweeps had an extremely slow settling time, as well as almost the double of rising times as the first two trials. Since in most of the aforementioned cases the overshoot was critical, it was decided to apply some dynamical friction in order to assess the differences. As a consequence, rising times were slowed down between these 2 and 5 aforementioned times compared to the underdamped (indeed, non-damped) conditions, but the overshoot remained almost the same one in all three cases, highlighting the enhancement. As a matter of fact, in these last graphs of the second session, the overshoot tendency improves with the muffle effect, having more damped responses.

Enhancement proposals for the controller

Aiming to shed light on enhancement proposals, it could be possible to include a Kd, to change the relation of Kp/Ki to slow down the loop rhythm as well as less aggressive and sudden or emulate the muffle effect with the controller constants depending also on the desires at the biological level (e.g. more velocity of movement, more precision and accuracy, less oscillations…).

Comparatives between the controllers from TA and MG

9 different trials were collected. 3 of them corresponded to a desired trajectory of +10º, leading to three vastly different transient responses and contrasted overshoots, having the second one (v2.0) the most sudden initial peak and concomitantly, the largest stimulation burst duration (100 µs) followed by the first one (95 µs) and the third one (40 µs). Apart from them, both versions of the muffled trials led to a smoother peak overshoot, and, ultimately, the trials conducted under ramp or sweep behaviors are extremely time-dilated and smooth in terms of stimulation burst duration increases.

What it does with the second controller accounting for the MG implant, results seem interestingly contrasted in the scenarios of the ramp and sweep if compared with the TA. Medial gastrocnemius is a muscle that is composed by a heterogeneous mixture of muscle fibers, making expectable the fact of finding more ripple in the responses. Indeed, in the extreme cases that forced the system to experience ramps and sweeps, the controller needed to act as a forward-backward player, trying to complete a controller cycle. However, in the cases of ±10º the responses are not that far from PID Controller 0 (TA), since the arch of trajectories was not that extensive (in fact, the overlapping angular arch is extremely small, little angle spans are simultaneously working, approximately 15-25% of the whole).

The open-loop architecture

The fact that the plateaus are so flat in all cases means that the Open Loop response lacking an error correction mechanism is overdamped, while in previous Closed Loop architecture, PID controllers' dynamics affected the response, being able to appreciate the transitory in the represented graphs.

Encountered problems

1) An inherent system's delay due to the fact that the plant lacks hysteresis and constantly looks backwards in timeframes, causing larger integrator windups and concomitantly, more aggressive hindlimb excursions in the agonist / antagonist muscle pair.

2) An increase in the settling time of the responses when the motion was descending, since there was no integrator control.

3) The integral term contribution was a trade-off since on the one hand accounted for a proper excursion control, but on the other hand, the response was faster, ultimately leading to the acceleration of fatigue. Following this point, rest periods between conducted trials were necessary, since they decrease the fatigue of the animal, and allow to perform more trials in each experimental assay. However, it also has a downside: the switching between fatigue and recovery periods may cause oscillations in the muscle properties that lead to instabilities and difficulties when controlling the gestures.

4) PID noise, which is mainly cause of the plant's dynamics, while the sensor barely presents, having a more stable behavior. However, it could have been removed, so this aspect has not been capital for the discussion here detailed.

5) SIMULINK fetches commands every 0.1 seconds, leading to a non-instantaneous response.

General study enhancement proposals

1) Adding a time-varying estimate of the input delay.

2) Transform the integrator of the plant to a leaky one that may reduce even more the transient overshoot, have an earlier integration windup and as a consequence, have a smoother time-varying hindlimb gestures.

3) It is evident the need of deploying a quicklier controller in terms of actuation timings in order to improve the response.

All of these improvements will be investigated in future experiments designed for more complex multiple muscle and multiple joint control. The present has been proper to demonstrate and validate the initial hypothesis: a single degree-of-freedom was accomplished in both directions of the rabbit's hindlimb trajectories.

5. CONCLUSION

This present study seeked to find applicability to eAXON prototypes produced by BERG to induce precise movements, aspect that in the past had not been accomplished. Here, the tested closed-loop controller and a network of eAXONs under a huge variety of trials all along two contrasted experimental sessions, showed that it is possible to control certain precise muscular gestures in an animal, mainly dorsiflexion and plantarflexion ones, limited to 1 degree-of-freedom in both senses of an agonist / antagonist muscle pair.

Therefore, the current thesis has made use of an electrical stimulation method based on implanted eAXONs, the ones that can rectify innocuous HF current bursts (1 MHz) delivered with textile band electrodes wrapped around the leg of the animal, that flow across muscles and ultimately, LF currents properly stimulate targeted muscle points through this eAXON injected microdevice. This all allowed to miniaturize the deployed system that in the past, led to such a bulky and problematic configuration. Entering more into detail, these eAXONs have been accurate when independently stimulating agonist / antagonist rabbit's hindlimb muscle pair of TA / MG. All in all, it has been realizable to deploy a closed-loop plant modulating stimulation bursts depending on the recorded angular variations cause of the eAXON implants and collected with the optical encoders located in the ankle joint of the rabbit.

As a conclusion, feedback control is capital to track gestures and make sure that an accurate amount of stimulus charge is delivered to the responsible muscular unit, preventing early fatigues. All in all, closed-loop architecture was useful when improving steady-state error as well as the transient behavior with respect to its open-loop homologue. Nonetheless, even though these preliminary assays are full of hope and settled down basis for future research, still further investigation on PID strategies for controlling trajectories in vertebrate individuals is needed [65].

All in all, it has been validated the objective of demonstrating the possibility to electrically rectify pulses applied by addressable microstimulators and, ultimately, control the angular trajectories they elicit thanks to a closed-loop controller designed in SIMULINK.

6. REFERENCES

[1] Forrest, G. P., Smith, T. C., Triolo, R. J., Gagnon, J. P., DiRisio, D., Miller, M. E., Murray, L., Davis, J. A., & Iqbal, A. (2007). Energy cost of the case Western reserve standing neuroprosthesis. Archives of physical medicine and rehabilitation, 88(8), 1074–1076.
doi: https://doi.org/10.1016/j.apmr.2007.05.011

[2] Fisher, L. E., Miller, M. E., Bailey, S. N., Davis, J. A., Jr, Anderson, J. S., Rhode, L., Tyler, D. J., & Triolo, R. J. (2008). Standing after spinal cord injury with four-contact nerve-cuff electrodes for quàdriceps stimulation. IEEE transactions on neural systems and rehabilitation engineering : a publication of the IEEE Engineering in Medicine and Biology Society, 16(5), 473–478.
doi: https://doi.org/10.1109/TNSRE.2008.2003390

[3] S. Jezernik, R. G. V. Wassink and T. Keller, "Sliding mode closed-loop control of FES controlling the shank movement," in IEEE Transactions on Biomedical Engineering, vol. 51, no. 2, pp. 263-272, Feb. 2004.
doi: 10.1109/TBME.2003.820393.

[4] Li, Z., Guiraud, D., Andreu, D., Gelis, A., Fattal, C., & Hayashibe, M. (2018). Real-Time Closed-Loop Functional Electrical Stimulation Control of Muscle Activation with Evoked Electromyography Feedback for Spinal Cord Injured Patients. International journal of neural systems, 28(6), 1750063.
doi: https://doi.org/10.1142/S0129065717500630

[5] H. J. Chizeck, P. E. Crago and L. S. Kofman, "Robust closed-loop control of isometric muscle force using pulsewidth modulation," in IEEE Transactions on Biomedical Engineering, vol. 35, 7, pp. 510-517, July 1988
doi: 10.1109/10.4579.

[6] Ch. Azevedo Coste, B. Sijobert, J. Froger, Ch. Fattal, Preliminary developments towards closed-loop FES-assistance of posture and gait, IFAC-PapersOnLine, Volume 48, Issue 20, 2015, 333-337, ISSN 2405-8963
doi: https://doi.org/10.1016/j.ifacol.2015.10.161.

[7] Loeb, G. E., Peck, R. A., Moore, W. H., & Hood, K. (2001). BION system for distributed neural prosthetic interfaces. Medical engineering & physics, 23(1), 9–18.
doi: https://doi.org/10.1016/s1350-4533(01)00011-x

[8] J. S. Ho et al., "Wireless power transfer to deep-tissue microimplants," Proc. Nat. Acad. Sci. USA, vol. 111, no. 22, pp. 7974–7979, May 2014. 7
doi: https://doi.org/10.1073/pnas.1403002111

[9] Sahin, M., & Pikov, V. (2011). Wireless microstimulators for neural prosthetics. Critical reviews in biomedical engineering, 39(1), 63–77
doi: https://doi.org/10.1615/critrevbiomedeng.v39.i1.50

[10] Seo, D., Carmena, J. M., Rabaey, J. M., Maharbiz, M. M., & Alon (2015). Model validation of untethered, ultrasonic neural dust motes for cortical recording. Journal of neuroscience methods, 244, 114–122.
doi: https://doi.org/10.1016/j.jneumeth.2014.07.025

[11] Ibrahim, A., Meng, M., & Kiani, M. (2018). A Comprehensive Comparative Study on Inductive and Ultrasonic Wireless Power Transmission to Biomedical Implants. IEEE sensors journal, 18(9), 3813–3826.
doi: https://doi.org/10.1109/JSEN.2018.2812420

[12] Chang, T. C., Weber, M. J., Charthad, J., Baltsavias, S., & Arbabian, A. (2018). End-to-End Design of Efficient Ultrasonic Power Links for Scaling Towards Submillimeter Implantable Receivers. IEEE transactions on biomedical circuits and systems, 12(5), 1100–1111.
doi: https://doi.org/10.1109/TBCAS.2018.2871470

[13] R. V. Taalla, M. S. Aren, A. Kaynak, and A. Z. Kouzani, ``A review on miniaturized ultrasonic wireless power transfer to implantable medical devices,'' IEEE Access, vol. 7, pp. 20922106, 2019
doi: 10.1109/ACCESS.2018.2886780

[14] Abdo, A., Sahin, M., Freedman, D. S., Cevik, E., Spuhler, P. S., & Unlu, M. S. (2011). Floating light-activated microelectrical stimulators tested in the rat spinal cord. *Journal of neural engineering*, *8*(5), 056012.
doi: https://doi.org/10.1088/1741-2560/8/5/056012

[15] H. Liu et al., "Flexible battery-less bioelectronic implants: Wireless powering and manipulation by near-infrared light," Adv. Funct. Mater., vol. 25, no. 45, pp. 7071–7079, Dec. 2015.
doi: 10.1002/adfm.201502752

[16] P. P. Mercier, A. C. Lysaght, S. Bandyopadhyay, A. P. Chandrakasan, and K. M. Stankovic, "Energy extraction from the biologic battery in the inner ear," Nature Biotechnol., vol. 30, 12, 1240–1243, Dec. 2012
doi: 10.1038/nbt.2394

[17] Becerra-Fajardo L, Schmidbauer M, Ivorra A (2017) Demonstration of 2 mm Thick Microcontrolled Injectable Stimulators Based on Rectification of High Frequency Current Bursts.
doi: 10.1109/TNSRE.2016.2623483

[18] Hunt, K. J., Gollee, H., & Jaime, R. P. (2001). Control of paraplegic ankle joint stiffness using FES while standing. Medical engineering & physics, 23(8), 541–555.
doi: https://doi.org/10.1016/s1350-4533(01)00089-3

[19] Holderbaum, W., Hunt, K. J., and Gollee, H. (2004). Robust discrete H∞ control for unsupported paraplegic standing: experimental results. Eur. J. Control 10, 275–284.
doi: 10.3166/ejc.10.275-284

[20] Y. Wei, J. Qiu, P. Shi and H. Lam, "A New Design of H -Infinity Piecewise Filtering for Discrete-Time Nonlinear Time-Varying Delay Systems via T–S Fuzzy Affine Models," in IEEE Transactions on Systems, Man, and Cybernetics: Systems, vol. 47, no. 8, pp. 2034-2047, Aug. 2017.
doi: 10.1109/TSMC.2016.2598785.

[21] Kobravi, H. R., and Erfanian, A. (2012). A decentralized adaptive fuzzy robust strategy for control of upright standing posture in paraplegia using functional electrical stimulation. Med. Eng. Phys. 34, 28–37.
doi: 10.1016/j.medengphy.2011.06.013

[22] L. A. Bernotas, P. E. Crago and H. J. Chizeck, "Adaptive Control of Electrically Stimulated Muscle," in IEEE Transactions on Biomedical Engineering, vol. BME-34, no. 2, pp. 140-147, Feb. 1987
doi: 10.1109/TBME.1987.326038.

[23] H. J. Chizeck, N. Lan, L. S. Palmieri and P. E. Crago, "Feedback control of electrically stimulated muscle using simultaneous pulse width and stimulus period modulation," in IEEE Transactions on Biomedical Engineering, vol. 38, no. 12, pp. 1224-1234, Dec. 1997
doi: 10.1109/10.137288.

[24] Ferrarin, M., Palazzo, F., Riener, R., & Quintern, J. (2001). Model-based control of FES-induced single joint movements. IEEE transactions on neural systems and rehabilitation engineering : a publication of the IEEE Engineering in Medicine and Biology Society, 9(3), 245–257.
doi: https://doi.org/10.1109/7333.948452

[25] Durfee W. K. (1989). Task-based methods for evaluating electrically stimulated antagonist muscle controllers. *IEEE transactions on bio-medical engineering*, *36*(3), 1989, 309–321. https://doi.org/10.1109/10.19852

[26] Meng, W, Liu, Q, Zhou, Z et al. (3 more authors) (2015) Recent development of mechanisms and control strategies for robot-assisted lower limb rehabilitation. Mechatronics, 31. pp. 132-145. ISSN 0957-4158
doi: https://doi.org/10.1016/j.mechatronics.2015.04.005

[27] R. Gaino, M. R. Covacic, M. C. M. Teixeira, et al, "Electrical stimulation tracking control for paraplègic patients using T–S fuzzy models,", May 2017, Fuzzy Sets & Systems, 201
doi: http://dx.doi.org/10.1016/j.fss.2016.06.005

[28] Qiu, S., Xu, R., Zhai, T., Fu, A., Xu, Q., Qi, H., Zhou, P., Zhang, L., Wan, B., Wang, W., Abboud, R., & Ming, D. (2013). Ant Colony Optimization Tuning PID Algorithm for Precision Control of Functional Electrical Stimulation. Biomedizinische Technik. Biomedical engineering
doi: https://doi.org/10.1515/bmt-2013-4017

[29] Arash Haghpanah, S., Farrokhnia, M., Taghvaei, S., Eghtesad, M., & Ghavanloo, E. (2022). Tracking ankle joint movements during gait cycle via control of functional electrical stimulation. Proceedings of the Institution of Mechanical Engineers, Part H: Journal of Engineering in Medicine, 236(2), 239-247.
doi: 10.1177/09544119211052365

[30] V. Nekoukar, A. Erfanian, "An adaptive fuzzy sliding-mode controller design for walking control with functional electrical stimulation: A computer simulation study," International Journal of Control Automation & Systems, vol. 9, no. 6, pp, 1124-1135, 2011.
doi: https://doi.org/10.1007/s12555-011-0614-4

[31] Isaly A, Allen BC, Sanfelice RG and Dixon WE (2021) Encouraging Volitional Pedaling in Functional Electrical Stimulation-Assisted Cycling Using Barrier Functions.Front. Robot. AI 8:742986.
doi: 10.3389/frobt.2021.742986

[32] E. F. Hodkin et al., "Automated FES for Upper Limb Rehabilitation Following Stroke and Spinal Cord Injury," in IEEE Transactions on Neural Systems and Rehabilitation Engineering, vol. 26, no. 5, pp. 1067-1074, May 2018
doi: 10.1109/TNSRE.2018.2816238.

[33] Rouhani Hossein, Same Michael, Masani Kei, Li Ya Qi, Popovic Milos R., PID Controller Design for FES Applied to Ankle Muscles in Neuroprosthesis for Standing Balance - Frontiers in Neuroscience, 11 (2017).
doi: 10.3389/fnins.2017.00347

[34] Lew B, Alavi N, Randhawa BK and Menon C (2016) An Exploratory Investigation on the Use of Closed-Loop Electrical Stimulation to Assist Individuals with Stroke to Perform Fine Movements with Their Hemiparetic Arm. Front. Bioeng. Biotechnol. 4:20.
doi: 10.3389/fbioe.2016.00020

[35] Frankel MA, Mathews VJ, Clark GA, Normann RA and Meek SG (2016) Control of Dynamic Limb Motion Using Fatigue-Resistant Asynchronous Intrafascicular Multi-Electrode Stimulation. Front. Neurosci. 13 September 2016.
doi: https://doi.org/10.3389/fnins.2016.00414

[36] Yoshida, K., & Horch, K. (1996). Closed-loop control of ankle position using muscle afferent feedback with functional neuromuscular stimulation. *IEEE transactions on biomedical engineering*, *43*(2), 167–176.
doi: https://doi.org/10.1109/10.481986

[37] Closed-loop functional optogenetic stimulation S. Srinivasan, B. E. Maimon, M. Diaz, H. Song, H. M.Herr, 2018
doi: https://doi.org/10.1038/s41467-018-07721-w

[38] Montazeri, M.; Yousefi, M.R.; Shojaei, K.; Shahgholian, G. Fast adaptive fuzzy terminal sliding mode control of synergisticmovement of the hip and knee joints (air-stepping) using functional electrical stimulation: A simulation study. Biomed. Signal Process. Control 2021, 66, 102445.
doi: 10.1016/j.bspc.2021.102445

[39] Lo, H. C., Hsu, Y. C., Hsueh, Y. H., & Yeh, C. Y. (2012). Cycling exercise with functional electrical stimulation improves postural control in stroke patients. *Gait & posture*, *35*(3), 506–510.
doi: https://doi.org/10.1016/j.gaitpost.2011.11.017

[40] Jezernik S, Wassink RG, Keller T. Sliding mode closed-loop control of FES: controlling the shank movement. IEEE Transactions on Bio-medical Engineering. 2004 Feb;51(2):263-272.
doi: 10.1109/tbme.2003.820393.

[41] Ward, T.; Grabham, N.; Freeman, C.; Wei, Y.; Hughes, A.-M.; Power, C.; Tudor, J.; Yang, K. Multichannel Biphasic Muscle Stimulation System for Post Stroke Rehabilitation. Electronics 2020, 9, 1156
doi: https://doi.org/10.3390/electronics9071156

[42] Downey, R. J., Cheng, T. H., Bellman, M. J., & Dixon, W. E. (2017). Switched Tracking Control of the Lower Limb During Asynchronous Neuromuscular Electrical Stimulation: Theory and Experiments. IEEE transactions on cybernetics, 47(5), 1251–1262.
doi: https://doi.org/10.1109/TCYB.2016.2543699

[43] H. Wang, G. Chai, X. Sheng and X. Zhu, "A programmable, multichannel, miniature stimulator for electrotactile feedback of neural hand prostheses," 2021 10th International IEEE/EMBS Conference on Neural Engineering (NER), 2021, pp. 1026-1029
doi: 10.1109/NER49283.2021.9441192.

[44] Multiscale computational model of Achilles tendon wound healing: Untangling the effects of repair and loading – K.Chen et al., December 14, 2018
doi: https://dx.doi.org/10.1371%2Fjournal.pcbi.1006652

[45] Intraoperative testing of passive and active state mechanics of spastic semitendinosus in conditions involving intermuscular mechanical interactions and gait relevant joint positions. S.Kaya, S.Bilgili, E.Akalan, A.Yucesoy, 16 April 2020
doi: https://doi.org/10.1016/j.jbiomech.2020.109755

[46] S.Mahadas, K.Mahadas, G.Hung - Biomechanics of the golf swing using OpenSim – February 2019
doi: https://doi.org/10.1016/j.compbiomed.2018.12.002

[47] M.E.Raabe, A.M.W Chaudhari - Biomechanical consequences of running with deep core muscle weakness, 23 January 2018
doi: https://doi.org/10.1016/j.jbiomech.2017.11.037

[48] Delp, S. L., Anderson, F. C., Arnold, A. S., Loan, P., Habib, A., John, C. T., Guendelman, E., & Thelen,D. G. (2007). OpenSim: open-source software to create and analyze dynamic simulations of movement. IEEE transactions on biomedical engineering, 54(11), 1940–1950.
doi: https://doi.org/10.1109/TBME.2007.901024

[49] Myers CA, Laz PJ, Shelburne KB, et al. Simulated hip abductor strengthening reduces peak joint contact forces in patients with total hip arthroplasty. J Biomech. 2019;93:18-27.
doi: 10.1016/j.jbiomech.2019.06.003

[50] Lee LF, Umberger BR. Generating optimal control simulations of musculoskeletal movement using OpenSim and MATLAB. PeerJ. 2016; 4:e1638. 2016 Jan 26.
doi: 10.7717/peerj.1638

[51] Daniel Shevitz, Brad Paden. Lyapunov Stability Theory of Nonsmooth Systems. IEEE Transactions on Automatic Control, Institute of Electrical and Electronics Engineers, 1994, 39 (9), pp.1910-1914.
doi: 10.1109/9.317122

[52] J. Ding, A. S. Wexler, and S. A. Binder-Macleod, "A predictive fatigue model. I. Predicting the effect of stimulation frequency and pattern on fatigue," IEEE Trans. Rehabil. Eng., vol. 10, no. 1, pp. 48–58, Mar. 2002.
doi: 10.1109/TNSRE.2002.1021586

[53] Z. Li, M. Hayashibe, C. Fattal, and D. Guiraud, "Muscle fatigue tracking with evoked EMG via recurrent neural network: Toward personalized neuroprosthetics," IEEE Comput. Intell. Mag.,9, 2, 38–46, May 2014.
doi: 10.1109/MCI.2014.2307224

[54] S. U. Yavuz, A. Şendemir-Ürkmez, and K. S. Türker, "Effect of gender, age, fatigue and contraction level on electromechanical delay," Clin. Neurophysiol., vol. 121, no. 10, pp. 1700–1706, Oct. 2010.
doi: 10.1016/j.clinph.2009.10.039.

[55] Cè, E., Rampichini, S., Agnello, L., Limonta, E., Veicsteinas, A., & Esposito, F. (2013). Effects of temperature and fatigue on the electromechanical delay components. Muscle & nerve, 47(4), 566–576.
doi: https://doi.org/10.1002/mus.23627

[56] R. J. Downey, M. Merad, E. J. Gonzalez, and W. E. Dixon, "The time-varying nature of electromechanical delay and muscle control effectiveness in response to stimulation-induced fatigue," IEEE Trans. Neural Syst. Rehabil. Eng., vol. 25, no. 9, pp. 1397–1408, Sep. 2017
doi: https://doi.org/10.1177/23259671211041591

[57] Becerra-Fajardo L, Ivorra A (2015) In Vivo Demonstration of Addressable Microstimulators Powered by Rectification of Epidermically Applied Currents for Miniaturized Neuroprostheses. e0131666.
doi: 10.1371/journal.pone.0131666

[58] Rouhani H, Same M, Masani K, Li YQ, Popovic MR. PID Controller Design for FES Applied to Ankle Muscles in Neuroprosthesis for Standing Balance. Front Neurosci. 2017;11:347. 2017 Jun 20.
doi: 10.3389/fnins.2017.00347

[59] Hunt, K. J., Gollee, H., and Jaime, R. P. (2001). Control of paraplegic ankle joint stiffness using FES while standing. Med. Eng. Phys. 23, 541–555.
doi: 10.1016/S1350-4533(01)00089-3

[60] Kobravi, H. R., and Erfanian, A. (2012). A decentralized adaptive fuzzy robust strategy for control of upright standing posture in paraplegia using functional electrical stimulation. Med. Eng. Phys. 34, 28–37.
doi: 10.1016/j.medengphy.2011.06.013

[61] Hunt, K. J., Munih, M., and de N Donaldson, N. (1997). Feedback control of unsupported standing in paraplegia-part I: optimal control approach. IEEE Trans. Rehabil. Eng. 5, 331–340.
doi: 10.1109/86.650287

[62] Munih, M., de N Donaldson, N., Hunt, K. J., and Barr, F. M. (1997). Feedback control of unsupported standing in paraplegia–part II: experimental results. IEEE Trans. Rehabil. Eng. 5, 341–352.
doi: 10.1109/86.650288

[63] H. Gollee, K. J. Hunt and D. E. Wood, "New results in feedback control of unsupported standing in paraplegia," in IEEE Transactions on Neural Systems and Rehabilitation Engineering, vol. 12, no. 1, pp. 73-80, March 2004
doi: 10.1109/TNSRE.2003.822765.

[64] Rouhani, H., Same, M., Masani, K., Li, Y. Q., & Popovic, M. R. (2017). PID Controller Design for FES Applied to Ankle Muscles in Neuroprosthesis for Standing Balance. Frontiers in neuroscience, 11, 347,
doi: https://doi.org/10.3389/fnins.2017.00347

[65] Schiaffino, Luciano & Tabernig, Carolina. (2013). Position control with PID regulation for a FES system: Preliminary results. Journal of Physics: Conference Series. 477.
doi: 10.1088/1742-6596/477/1/012039.

[66] Eladly, A., Del Valle, J., Minguillon, J., Mercadal, B., Becerra-Fajardo, L., Navarro, X., & Ivorra, A. (2020). Interleaved intramuscular stimulation with minimally overlapping electrodes evokes smooth and fatigue resistant forces. Journal of neural engineering, 17(4), 046037.
doi: https://doi.org/10.1088/1741-2552/aba99e

[67] Ivorra, A., Becerra-Fajardo, L., & Castellví, Q. (2015). In vivo demonstration of injectable microstimulators based on charge-balanced rectification of epidermically applied currents. Journal of neural engineering, 12(6), 066010.
doi: https://doi.org/10.1088/1741-2560/12/6/066010

7. List of figures and tables

- **Figures**

- **Tables**

8. SUPPLEMENTARY INFORMATION

A secondary objective of the current thesis was the simulation and analysis of a musculoskeletal model in an in-silico interface, so that one could gamify with a virtual animal in which certain assessments of focused muscles, trajectories and responses upon the application of certain load forces or current bursts were obtained, without the need of being in a surgical in-person set-up. In this context, OpenSim is used for all this, offering tracking algorithms (CMC), actuators (muscles) and analyses (muscle-induced accelerations). Its GUI offers tools for viewing models, editing muscles, generating muscle-actuated simulations and plotting results. However, a clear downside is the fact that it has limited resources for quick design and control of dynamical systems, as well as a complex integration with the controller GUI from SIMULINK, aspect that ultimately leads to the failure of results obtention in this objective. However, since this framework may serve as future lead of research, it has been decided to include it as supplementary information.

OpenSim virtual model

The chosen model corresponded to a mouse [45], the one that needed to be scaled to a different size (specifically augmented by a scaling factor of 1.5) and diameter of fibers, so that in the end, the model under study was as similar to a rabbit as possible. Once here, a validation procedure was needed in order to test whether the preconditioning and scaling was approached in a successful way. Therefore, a main hypothesis was to be claimed: muscular forces are distributed following an optimization criterion, minimizing activations. Slack tendon lengths were empirically fine-tuned. However, this may result in regions where the muscle operates on the force-length curve not realistically at all. In this context, dynamical MATLAB files accounting for a dorsiflexion and plantarflexion were created, and what it could be said about the results in the resulting forces file (.sto) was that there were muscular forces that seemed consistent with the joint moments that were needed to develop these dorsiflexion and plantarflexion gestures. Apart from that, the activations from most of muscles were small, meaning that they were far from being activated at 100% when performing the movement, which seems reasonable enough too.

Forward Dynamics simulation

The muscle forces are defined by dynamics and integrate control inputs (e.g. muscle excitations, torque generators) varying their response. These dynamics allows to dispose of the forces that act upon the model, calculate the joint moments and ultimately, accelerations thanks to what is known as multibody dynamics.

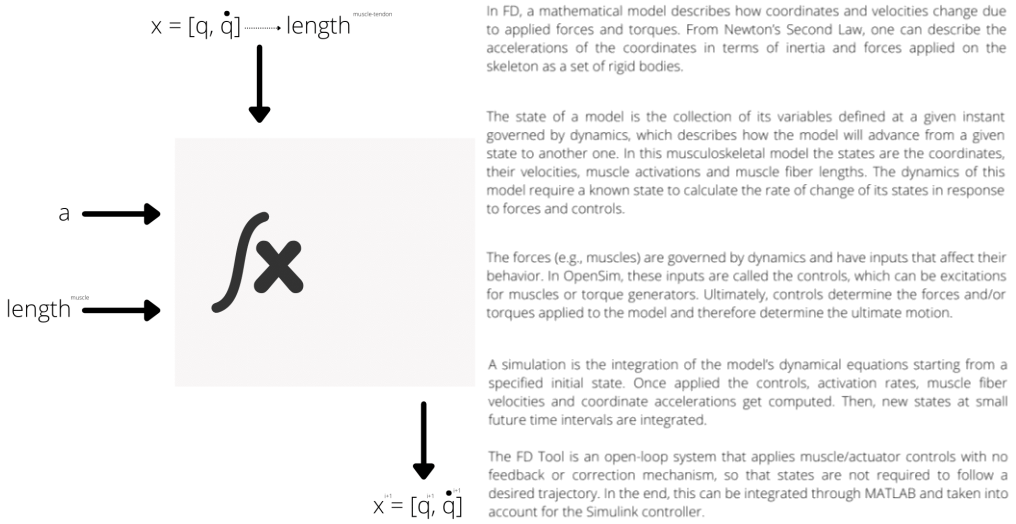

Fig. 1 from Supplementary Information:
Infographic of the basic OpenSim flowchart when performing Forward Dynamics computations

Integration with MATLAB Simulink API

As a limitation of the current thesis, and a lead for future improvement, is the implementation of the created OpenSim musculoskeletal model and its Forward Dynamics framework with the MATLAB Simulink environment by means of the so-called S-Function, which may allow to change plant's parameters (e.g. Integration solver, error tolerance) aiming to adapt to problem specifications. Pursuing this link, S-functions are System-functions that extend Simulink possibilities by means of a specific computer language describing blocks in C, C++ or even Fortran. These S-functions are dynamically associated subtasks that MATLAB itself can load and compile. Its API allows to interact so similarly as a built-in function would do. The main goal of a S-Function is to integrate the neural command, musculotendon dynamics, the geometry and multibody dynamics into a single routine. This all may allow to make use of a Forward Dynamics simulation performing certain trajectories, link them all as an input of the Simulink block diagram error function, and spare time and experimental sessions, since currently most of results depend on laboratory trials.

Functioning of an S-function: OpenSim Forward Dynamics

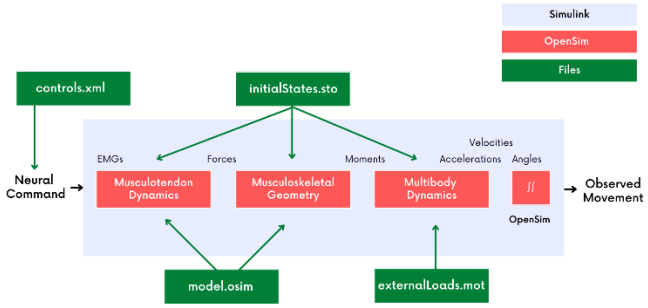

Fig. 2 from Supplementary Information:
Infographic of the S-function functioning

OpenSim validation for future research

Aiming to validate the obtained model, the maximum force in MG was collected with a value of 21.55 N. Indeed, comparing this force amount with the one found in the literatura, when MG was stimulated around its motor point in [66], its maximum twitch force was approximately of 4 N, which translated to torque, represents around 0.4 N.m. Since motor point is stimulated, one could assume that this one was the maximum force to be obtained in a twitch. However, tetanization may occur at much larger units (naturally 5-10 times bigger [67]). This similarity in values for the MG peak forces allowed to smoothly validate the model conditioning and scaling.

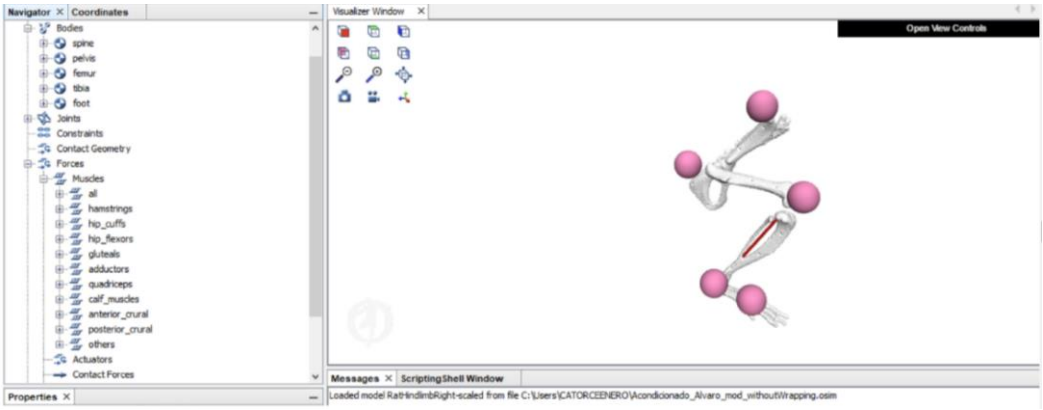

Fig. 3 from Supplementary Information:
Interface from OpenSim with the scaled, conditioned and constructed model of the rabbit's hindlimb

As a conclusion, as already stated, the usage of the constructed rabbit's musculoskeletal model has been purely anecdotal, since only visual results have been valuable for future research. However, having clear the flowchart with which to proceed, beginning with the utilization of the aforeshown constructed model, and continuing with the S-function link among SIMULINK and OpenSim, controlling the C++ code intertwining both interfaces, a promising research line could make a plot-twist of this current thesis limitation: accomplish a successful in-silico model that may reduce laboratory and surgical times in detriment of the experimentation and assessment of the same animal under equal conditions in a fiction way.

Access to the constructed model and the framework for the S-function
Representative video from an experimental session

https://drive.google.com/drive/folders/1x630zansY6elyU0AtEAM1FlsZZfsCzb-?usp=sharing